FROM THE DEPARTMENT OF RADIATION PHYSICS (DIRECTOR: PROF. K. LIDÉN),
UNIVERSITY OF LUND, SWEDEN.

DIGITAL STEREOSCINTIGRAPHIC EXPERIMENTS WITH A GAMMA-CAMERA

by

E. INGEMAR LARSSON

A number of ideas have been presented in the literature about the problems encountered in distinguishing over-lapping information from the information of interest in gamma-camera scintigraphy. FREEDMAN (1970) proposed a digital method very similar to the method described in the present work. MUEHLLEHNER's (1970, 1971) technique is based on analogue read-out, but is otherwise principally the same. Theoretical considerations around this problem are presented by CASSEN (1968) and MCAFFE & MOZLEY (1969). The present work is also based in part on the longitudinal section-scanning method described by KUHL & EDWARDS (1968). All previously described methods for three-dimensional investigations with the gamma-camera, except that of CHARKES & SOMBURANASIN (1968), however, require the use of quite different equipment than is ordinarily employed, thus eliminating the possibility of carrying out static or dynamic examinations with conventional depth-response. This is also the case with the methods described by ANGER (1968) and MIRALDI & DICHIRO (1970).

Submitted for publication 21 June 1971.

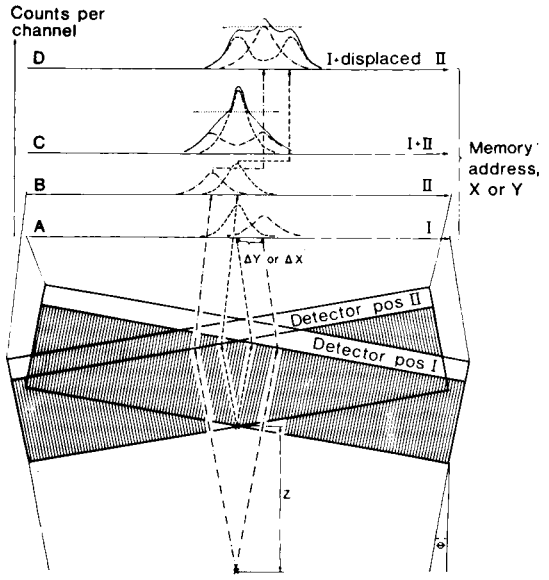

Fig. 1. Operating principle for stereoscintigraphy with conventional gamma-camera equipment and digital storage facilities. Sections A and B: PSF from two sources with detector in positions I and II, respectively. Section C: Sum of PSF in sections A and B. Section D: Sum of PSF in sections A and B with address-displacement as shown by arrows between sections B and D.

Method. A number of experiments which have been carried out for evaluating the stereoscintigraphic or tomographic possibilities with conventional gamma-camera equipment and digital storage facilities are described in the present work. (Nuclear Chicago: Pho Gamma III. Intertechnique: Bloc d'exploration, BM 96 B, 4096 word-memory; two Codeur d'amplitude, CA 13 B; Unité de visualisation, RG 96; Calculateur intermédiaire, RG 23.) The operating principle is illustrated in Fig. 1. At the bottom of this figure there are two point-sources having an internal distance of z. These two sources are first detected by the gamma-camera crystal with its parallel-hole collimator in position I. This means that the central axis of the detector deviates with an angle Θ from the normal direction of view. The photons from the upper source will be detected by the centre of the crystal and will also be counted in the centre of the memory, which is illustrated with the point-spread function (PSF) indicated by the dashed curve in section A of Fig. 1. Photons from the lower point-source will be counted in channels the mean address of which deviates ΔX or ΔY, which is proportional to $z \cdot \sin \Theta$, from the centre of the memory, as is illustrated by the dashed-dotted PSF in section A. This point-source will also be detected with a poorer resolution-distance as a result of the poorer imaging properties of the parallel-hole collimator for sources lying at a greater distance (Anger 1964, Larsson & Lidén 1969).

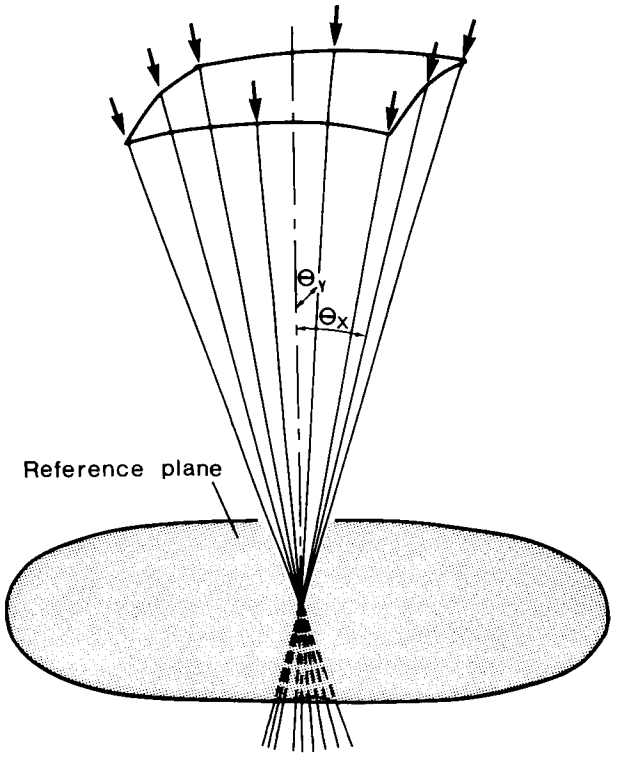

Fig. 2. Three-dimensional illustration of the direction of view for the central axis of the detector in eight elementary images. The angles of inclination are Θ_X and Θ_Y.

With the detector in position II, the upper source will still be seen by the centre of the detector and will be registered in the centre of the memory. Photons from the lower point-source, however, will be displaced to the left in the memory compared to position I (section B). Views Nos I and II in sections A and B are stored separately on magnetic tape. They can afterwards be summed into the solid line in section C without any address-modification. Using a certain suppression-level, indicated by the dotted line in the figure, we can now display channels containing pulses the main part of which is obtained from the upper point-source.

The solid line in section D also represents a sum of views Nos I and II, but all addresses in view No. II are shifted in proportion to $z \cdot \sin \Theta$, as indicated by the arrows from section B to section D. The PSF from the upper source is therefore suppressed or blurred into the separated PSF indicated by the broken line in the same way as the lower source in section C. The view of the lower source is enhanced because the dashed-dotted PSF from sections A and B coincide in the memory.

The views in sections A and B can, of course, be viewed with a stereoscope (CHARKES & SOMBURANASIN 1968), giving a subjectively percepted three-dimensional image. Using the digital treatment illustrated here, we can make use of any desired angle of inclination and also extend it in several azimuths in order to avoid false summation of multiple sources as mentioned by MCAFFE & MOZLEY (1969). The size of the angles is partly limited by the reduction of the field of view at greater distances from the collimator.

It is apparent from Fig. 1 that the effect of the earlier explained suppression, or blurring, is greater the better the resolution one can achieve, because the PSF from different depths will be better differentiated in all sections of the figure. The blurring effect in the planes which are out of focus can also be regarded as a low pass-filtering of the spatial frequency-spectrum, i.e. a removal of high-frequency components.

The problem of selecting a rotation-centre close to the organ being investigated is solved by using an index which is mounted in the centre of the collimator. This index points towards the same point on the patient or the phantom in all the individual elementary images. The phantom, or patient, must therefore also normally be moved between each exposure.

Fig. 2 shows three-dimensionally how the angle of inclination is selected in eight different elementary views. Photons from any point in the shaded plane, hereafter called the reference-plane, receive the same memory-addresses in all the individual images, when using a small angle of inclination. This means that the best focus is achieved in this plane when the elementary images are added without address-modification.

Results

Focusing to any plane other than the reference-plane can be performed using different address-displacements when the elementary images are added. This is illustrated in Fig. 3, shown in the isometric-display fashion. In Fig. 3 a and b, four cobalt-57 point-sources are placed in the reference-plane and in Fig. 3 c and d the position of the sources is 12 cm below the reference-plane. Fig. 3 a and c are focused on this plane simply by adding all eight elementary images together without any address-displacement.

It is possible to focus to the point-sources 12 cm below the reference-plane as shown in Fig. 3 b and d if a certain address-modification is applied when the elementary images are added. In Fig. 3 b the individual point-spread functions from the eight elementary images are displayed slightly separated and suppressed with a factor of 8, as compared to Fig. 3 a. In Fig. 3 d, however, the eight PSF from the elementary images coincide in the memory and the resultant images

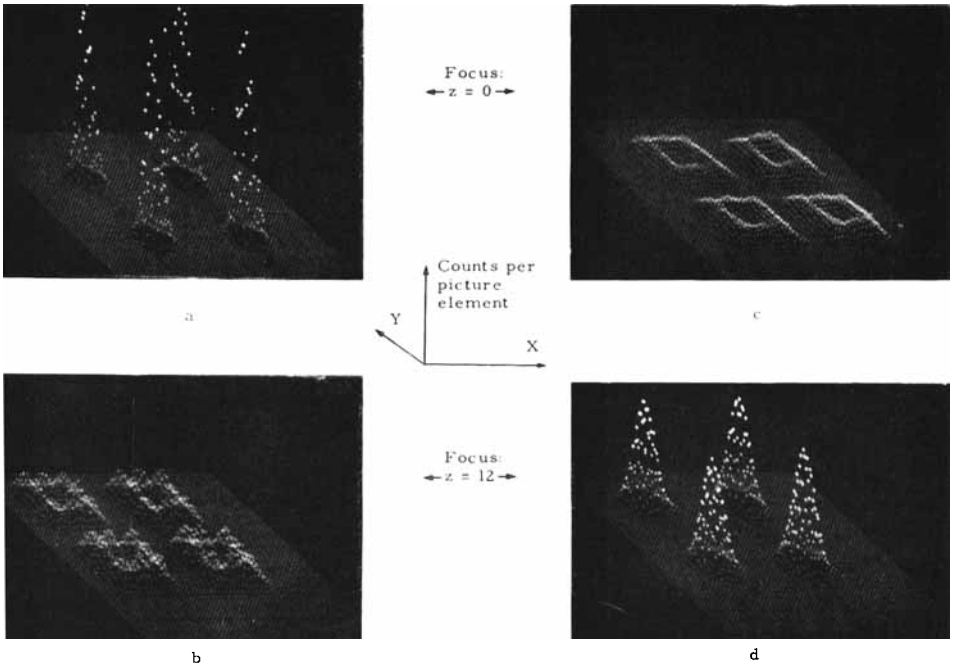

Fig. 3. Isometric display of point-sources at two different distances. a) and d) Sources in plane of best focus. b) Sources 12 cm above plane of best focus. c) Sources 12 cm below plane of best focus.

are therefore enhanced as compared to Fig. 3 c. The angle of inclination in this experiment is 10°.

Eight separate elementary images (B—I) are illustrated in Fig. 4 a, together with a view in the centre (A) taken without any inclination of the detector, i.e. with conventional depth-response. Three digits, '0', '7' and '14', drawn with technetium-99^{m} solution, are placed in the reference-plane, and at 7 and 14 cm below that plane, respectively. The eight minutes' exposure-time for the conventional view is now replaced by a one-minute exposure of each of the eight elementary images. In this case the angle of inclination is 20°. This relatively large angle makes it easier to see the differences between the separate elementary images, giving at the same time a more marked tomographic effect. There is a slight distortion of the projected plane when using this angle. This distortion also limits the angle of inclination in this technique, a limitation which does not exist when using a collimator with parallel-holes inclined in relation to the central axis of the detector (Freedman 1970, McAffe & Mozley 1969,

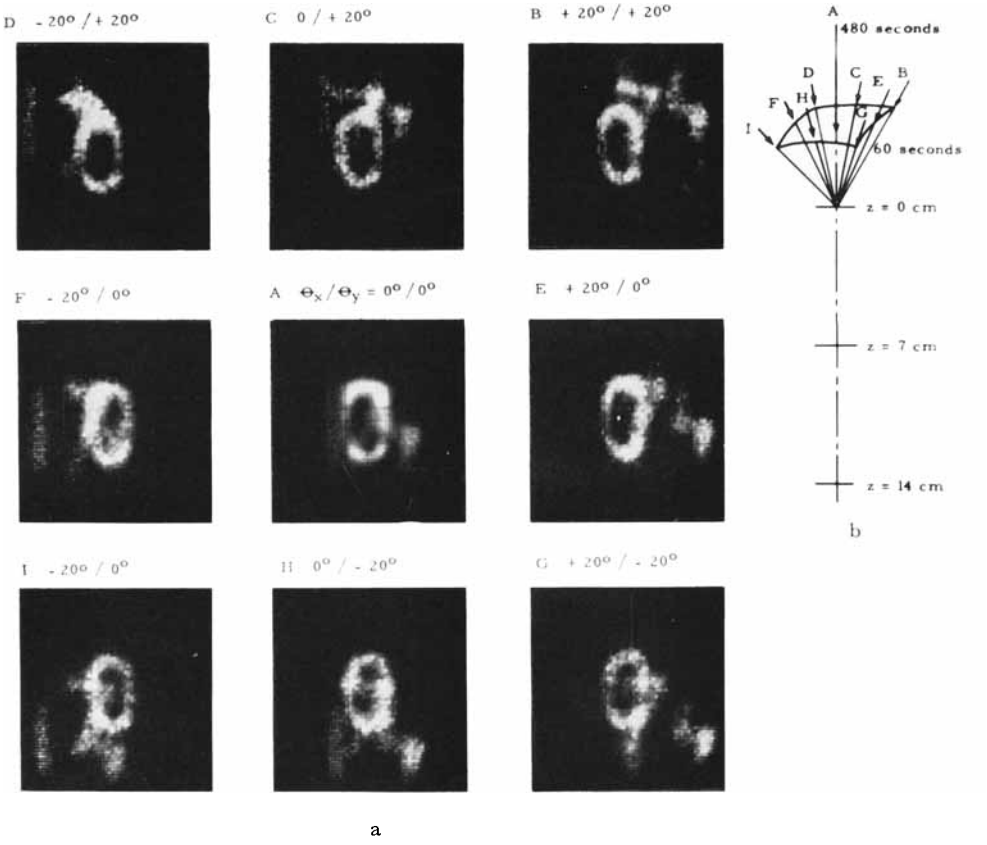

Fig. 4. Stereoscintigraphy of three digits, '0', '7' and '14', drawn with technetium solution and placed 0, 7 and 14 cm below the reference-plane, respectively. a) Illustration of the differences in the elementary images, (B-I). For purpose of comparison, image A is taken without inclination. b) Directions of detector and exposure-times for the eight elementary images and image A.

MUEHLLEHNER 1970, 1971). The necessity of working at a greater distance from the collimator, thereby degrading the overall resolution, is also a limiting factor when setting the angle of inclination.

When the elementary images in Fig. 4 a are added, it is, however, possible to enhance the contrast in the planes selected for best focus because the information from other depths is blurred. Identification of the different numbers from the planes selected is possible in Fig. 5 a, b and c.

For purposes of comparison it is here shown that it might not always be necessary to use all of the eight elementary images, as in Fig. 5 a, b and c; only four are used in Fig. 5 d, e and f. In these four elementary images it should be

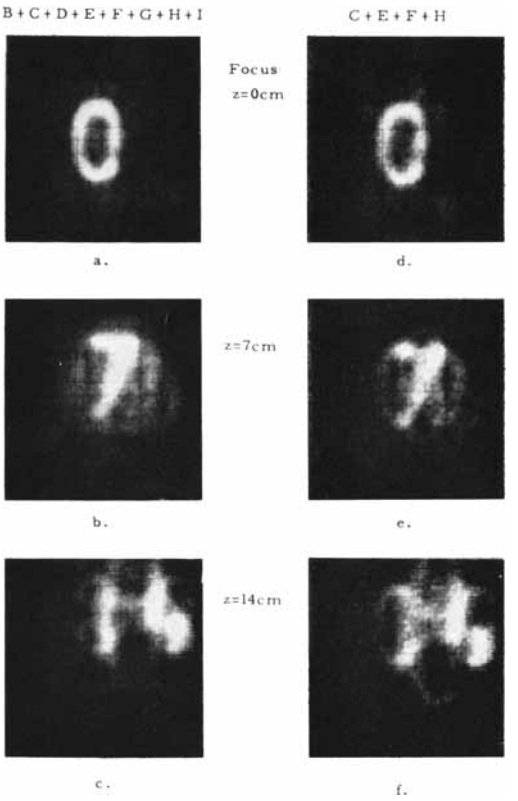

Fig. 5. Summation of the elementary images in fig. 4. Sum of the eight elementary images with a) '0' in plane of best focus (reference-plane), b) '7' in plane of best focus (7 cm below the reference-plane), and c) '14' in plane of best focus (14 cm below the reference-plane). d), e) and f) The same as for a), b) and c), respectively, but only four of the elementary images are used.

possible to compensate for the distortion of the projected plane mentioned earlier, when the angle of inclination is large. This could be done by a slight adjustment of the gain along the x- or y-axis, respectively, although this is a complicating factor which has not been used here. Better results are obtained from this comparison when more elementary images are used, and distortion of the kind mentioned earlier is negligible.

Fig. 6 illustrates that it is more difficult to achieve contrast-enhancement with this technique when looking for a region with lower activity-concentration than its surroundings. The liver-phantom in Fig. 6 has a simulated, non-active lesion placed as illustrated in the cross-sectional side-view of the phantom. Quantitative information is presented in the lower row of views as isocount-levels at 95, 90, 85, 80 and 75 % of the maximum. These levels are produced using repeated exposures on the same polaroid film and calculated settings on the dial determining the suppression-level on the RG 96-unit. To overcome the statistical

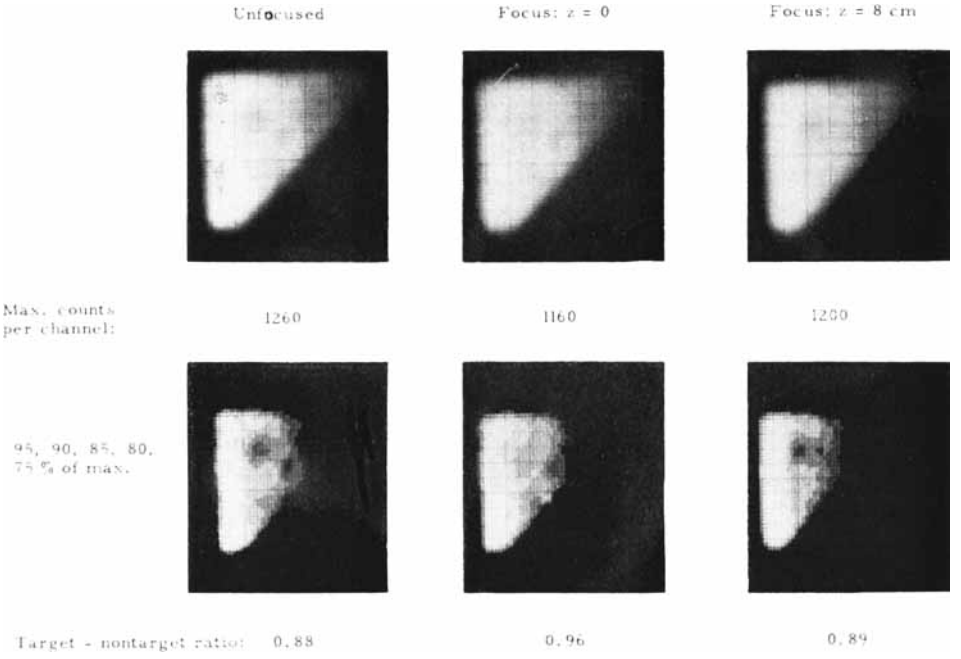

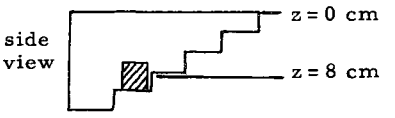

Fig. 6. Deep-lying simulated non-active lesion in a liver-phantom. E = 140 keV. $\Theta = \pm 10°$.

fluctuations along these levels, a nine-element smoothing-matrix is applied with the aid of the tape recorder RG 23 (LARSSON 1970). The conventional unfocused view has a target-to-non-target ratio of 0.88. Nothing can be said from the unfocused view alone about the depth of the simulated lesion. From the stereoscintigram with focusing to the surface, we get the information that it is not close to the surface, because it has a poorer target-to-non-target ratio. Focusing to the 8 cm depth gives the actual position of the simulated lesion, because this gives the same target-to-non-target ratio as obtained in the unfocused view. This focusing has, however, very little influence on the maximum number of counts, as this maximum is already from the beginning spread out over a large number of channels. This lack of contrast-enhancement can also be explained by the fact that the low pass-filtering has no effect on the d.c.-component in the spatial frequency-spectrum, or little influence on the low frequency-components.

Discussion

When applying this method on patients, it is desirable to take a view with the conventional depth-response. Although this increases the examination-time by a factor of 2, the whole procedure with readjustments of patient- and detector-position can be carried out without making undue demands on the patient.

It has been mentioned that a good resolution is of great importance when applying this or other, similar tomographic techniques. If the spatial frequency-spectrum contains only low-frequency components, the low pass-filtering will have little or no effect, as the high-frequency components have already been removed at earlier stages. This means that the visibility of the details will be poor in the plane of best focus also, as well as above or below this plane. The poor high-frequency response of all types of imaging devices of this kind complicates tomographic investigations in nuclear medicine. ANGER (1969) has achieved a better resolution by using a converging collimator. Extremely good resolution can be achieved with the pinhole-collimator at small distances (LARSSON & LIDÉN 1969), where sensitivity is also highest. These properties could also be used for tomographic purposes as noticed by BECK & ANGER (1969).

Acknowledgements

This work was supported by grants from John and Augusta Persson's Foundation for Medical Research, Karlskrona, Sweden. The author wishes to express his sincere gratitude to Prof. K. Lidén for fruitful discussions throughout the work.

SUMMARY

A simple and cheap method for stereoscintigraphy using conventional gamma-camera equipment and digital storage-facilities is described. Some experimental results are presented and discussed.

ZUSAMMENFASSUNG

Eine einfache und billige Methode für Stereoscintigraphie unter Anwendung einer konventionellen Gamma-Kamera-Ausrüstung und einem digitalen Speicher wird beschrieben. Einige experimentelle Ergebnisse werden gezeigt und besprochen.

RÉSUMÉ

Description d'une méthode simple et peu coûteuse pour faire une stéréoscintigraphie au moyen d'un équipement de gamma-caméra ordinaire et d'un équipement de stockage de données numériques. L'auteur présente quelques résultats expérimentaux et les examine.

REFERENCES

ANGER H. O.: Multiplane tomographic gamma-ray scanner. *In:* Medical radioisotope scintigraphy I, p. 203. IAEA, Vienna 1969.

— Scintillation camera with multichannel collimators. J. nucl. Med. 5 (1964), 515.

BECK R. N. and ANGER H. O.: Discussion. *In:* Medical radioisotope scintigraphy I, p. 216. IAEA, Vienna 1969.

CASSEN B.: Image formation by electronic cross-time correlation of signals from angular ranges of unfocused collimating channels. *In:* Medical radioisotope scintigraphy I, p. 107. IAEA, Vienna 1969.

CHARKES N. D. and SOMBURANASIN R.: Stereoscintigraphy. J. nucl. Med. 9 (1968), 494.

FREEDMAN G. S.: Tomography with a gamma camera. J. nucl. Med. 11 (1970), 602.

KUHL D. E. and EDWARDS R. Q.: Image separation radioisotope scanning. Radiology 80 (1963), 653.

LARSSON I.: Digital behandling och presentation av gammakamerabilder. (In Swedish.) Nord. Med. 83 (1970), 734.

— and LIDÉN K.: Resolution components and differential linearity of gamma camera. *In:* Medical radioisotope scintigraphy I, p. 111. IAEA, Vienna 1969.

MCAFFE J. G. and MOZLEY J. M.: Longitudinal tomographic radioisotopic imaging with a scintillation camera: theoretical considerations of a new method. J. nucl. Med. 10 (1969), 654.

MIRALDI F. and DICHIRO G.: Tomographic techniques in radioisotope imaging with proposal of a new device: the tomoscanner. Radiology 94 (1970), 513.

MUEHLLEHNER G.: Rotating collimator tomography. J. nucl. Med. 11 (1970), 347.

— A tomographic scintillation camera. Phys. in Med. Biol. 16 (1971), 87.